Superoxide Reductase from *Desulfoarculus baarsii*: Identification of Protonation Steps in the Enzymatic Mechanism†

Vincent Nivière,*,‡ Marcel Asso,§ Claire O. Weill,‡ Murielle Lombard,‡ Bruno Guigliarelli,§ Vincent Favaudon,⊥ and Chantal Houée-Levin#

Laboratoire de Chimie et Biochimie des Centres Redox Biologiques, DRDC-CEA/CNRS/Université Joseph Fourier, 17 Avenue des Martyrs, 38054 Grenoble Cedex 9, France, Unité de Bioénergétique et Ingénierie des Protéines, UPR 9036, CNRS, 31 Chemin J. Aiguier, 13402 Marseille Cedex 20, France, INSERM U 350, Institut Curie-Recherche, Bâtiment 112, Centre Universitaire 91405 Orsay Cedex, France, Laboratoire de Chimie Physique, CNRS/Université Paris-Sud, Bâtiment 350, Centre Universitaire 91405 Orsay Cedex, France

Received September 19, 2003; Revised Manuscript Received November 13, 2003

ABSTRACT: Superoxide reductase (SOR) is a metalloenzyme that catalyzes the reduction of $O_2^{\bullet-}$ to H_2O_2 and provides an antioxidant mechanism in some anaerobic and microaerophilic bacteria. Its active site contains an unusual mononuclear ferrous center (center II). Protonation processes are essential for the reaction catalyzed by SOR, since two protons are required for the formation of H_2O_2. We have investigated the acido-basic and pH dependence of the redox properties of the active site of SOR from *Desulfoarculus baarsii*, both in the absence and in the presence of $O_2^{\bullet-}$. In the absence of $O_2^{\bullet-}$, the reduction potential and the absorption spectrum of the iron center II exhibit a pH transition. This is consistent with the presence of a base (BH) in close proximity to the iron center which modulates its reduction properties. Studies of mutants of the closest charged residues to the iron center II (E47A and K48I) show that neither of these residues are the base responsible for the pH transitions. However, they both interact with this base and modulate its pK_a value. By pulse radiolysis, we confirm that the reaction of SOR with $O_2^{\bullet-}$ involves two reaction intermediates that were characterized by their absorption spectra. The precise step of the catalytic cycle in which one protonation takes place was identified. The formation of the first reaction intermediate, from a bimolecular reaction of SOR with $O_2^{\bullet-}$, does not involve proton transfer as a rate-limiting step, since the rate constant k_1 does not vary between pH 5 and pH 9.5. On the other hand, the rate constant k_2 for the formation of the second reaction intermediate is proportional to the H^+ concentration in solution, suggesting that the proton arises directly from the solvent. In fact, BH, E47, and K48 have no role in this step. This is consistent with the first intermediate being an iron(III)-peroxo species and the second one being an iron(III)-hydroperoxo species. We propose that BH may be involved in the second protonation process corresponding to the release of H_2O_2 from the iron(III)-hydroperoxo species.

Superoxide radical ($O_2^{\bullet-}$) is the univalent reduction product of molecular oxygen and belongs to the group of the so-called reactive oxygen species, also including hydrogen peroxide, peroxynitrite, and hydroxyl radical (*1*). Detoxification of $O_2^{\bullet-}$ is a crucial part of the cellular antioxidant defense mechanisms which allows the cell to grow in the presence of molecular oxygen. Two enzymatic systems are able to catalyze elimination of superoxide. The first system involves superoxide dismutases (SOD)[1] (*2*). SODs were characterized more than 30 years ago and are present in erythrocytes and in most cells and tissues. Four classes of SODs have been characterized so far, depending on the nature of the metal on their active site (*2*). They all catalyze the same reaction, e.g., the dismutation of superoxide radical to hydrogen peroxide and molecular oxygen:

$$O_2^{\bullet-} + O_2^{\bullet-} + 2H^+ \rightarrow H_2O_2 + O_2$$

A few years ago, some specific anaerobic and microaerophilic bacteria were shown to utilize an alternative enzymatic activity to eliminate superoxide (*3*, *4*). The enzyme, a small metalloprotein of ca. 14 kDa, catalyzes the reduction of $O_2^{\bullet-}$

† This work was supported by grants from the CNRS, programme Physique et Chimie du Vivant (V.N.), from the Ministère de la Recherche, programme de Recherche Fondamentale en Microbiologie et Maladies Infectieuses et Parasitaires (V.N.) and from the Institut National de la Santé et de la Recherche Médicale (V.F.). C.W. acknowledges a fellowship from the CEA, programme "Toxicologie Nucléaire".

* To whom correspondence should be addressed. Tel.: 33-4-38-78-91-09; fax: 33-4-38-78-91-24; e-mail: vniviere@cea.fr.

‡ DRDC-CEA/CNRS/Université Joseph Fourier.

§ UPR 9036, CNRS.

⊥ INSERM U 350, Institut Curie-Recherche.

CNRS/Université Paris-Sud.

[1] Abbreviations: SOD, superoxide dismutase; SOR, superoxide reductase; Dfx, desulfoferrodoxin; Nlr, neelaredoxin.

10.1021/bi035698i CCC: $27.50
Published on Web 12/24/2003

into H_2O_2 without production of oxygen, and was thus named superoxide reductase (SOR):

$$O_2^{\bullet-} + SOR_{(Fe2+)} + 2H^+ \rightarrow H_2O_2 + SOR_{(Fe3+)}$$

$$SOR_{(Fe3+)} + 1e^- \rightarrow SOR_{(Fe2+)}$$

$$O_2^{\bullet-} + 1e^- + 2H^+ \rightarrow H_2O_2$$

The active site of SOR consists of an Fe^{2+} center (center II) in an unusual [His_4 Cys_1] square pyramidal pentacoordination (*5*). SOR reacts specifically at a nearly diffusion-controlled rate with $O_2^{\bullet-}$, generating H_2O_2 and the oxidized active site, the Fe^{3+} center II (*3*). The electrons involved in the reaction can be provided to the oxidized center II by rubredoxin in the case of sulfate reducing bacteria (*6*) or by NAD(P)H-dependent cellular reductases in the absence of rubredoxin (*3*). Although this reduction step could be relatively slow, it has been proposed that the limiting step for SOR turnover would be the diffusion-controlled reaction of reduced center II with superoxide, taking into account a steady-state superoxide concentration in the cell of about 10^{-9} M (*6*).

Three classes of SOR have been described, depending on whether their sequence contains or not a small N-terminal domain that binds a desulforedoxin-like iron center (center I). Center I consists of an Fe^{3+} ion chelated by four cysteinyl sulfur ligands (*5*). However, when present in the protein, center I does not seem to be involved in SOR activity, and its function is still a matter of discussion (*7*−*9*).

The so-called homodimeric desulfoferrodoxin (Dfx) proteins are prototype of the first class of SOR. Dfx have been identified in *Desulfovibrio desulfuricans* (*10*), *Desulfovibrio vulgaris* Hildenborough (*11*), and *Desulfoarculus baarsii* (*3*). Dfx contains the iron centers I and II and has been structurally characterized (*5*). The homotetrameric neelaredoxin protein (Nlr) such as from *Pyrococcus furiosus* (*4*, *12*, *13*), *Archaeoglobus fulgidus* (*14*), and *Desulfovibrio gigas* (*15*) are the best representative of the second class of SOR. Each polypeptide contains only one iron center (center II), structurally almost identical to the iron center II of Dfx. Nlrs present large sequence homologies with the C-terminal domain of Dfx, but differs by the absence of the second domain to bind the iron center I (*12*). A third type of SOR, with high sequence homology to Dfx, but containing a single iron center (center II), has been isolated in the spirochete *Treponema pallidum* (*7*, *8*). The protein apparently contains the N-terminal domains, but lacks three of the four cysteine residues involved in the chelation of the iron center I. No structural data are available for this class of SOR.

Pulse radiolysis studies on SORs have shed light on their enzyme mechanism (*9*, *16*−*20*). It is now generally agreed that the reaction of $O_2^{\bullet-}$ with the reduced iron center II proceeds through an inner-sphere mechanism. The first step of the reaction consists of a bimolecular reaction of SOR with $O_2^{\bullet-}$ in a nearly diffusion-controlled process (10^9 M^{-1} s^{-1}). Site-directed mutagenesis studies highlighted the role of the K48 residue in this process. Actually, K48, a strictly conserved charged residue as close as 6−7 Å to the reduced iron center II (*5*, *12*), provides an electrostatic attraction of superoxide anion to the active site. In all the enzymes studied, the primary reaction intermediate exhibited a broad absorption band at 600 nm and was proposed to be an iron(III)-peroxide species. That the active site of SOR can indeed stabilize transiently such species was further demonstrated by resonance Raman and Mössbauer spectroscopies in the case of the *D. baarsii* enzyme (*21*, *22*) and modeled by DFT calculation (*23*). However, depending on the enzyme studied, the subsequent steps of the catalytic cycle differ. In the SORs from *D. vulgaris* Hildenborough (*9*, *16*, *20*) and *A. fulgidus* (*19*), the first intermediate turns out to be protonated to give directly the final product of the reaction, the oxidized center II and presumably H_2O_2. In the case of SORs from *D. baarsii* (*17*) and *T. pallidum* (*18*), an additional reaction intermediate has been identified, with a spectrum different from that of both the first intermediate and the final product of the reaction, the oxidized center II. This second intermediate is converted into the final products, H_2O_2 and the oxidized iron center II, possibly with the help of the strictly conserved E47 residue (*21*). This residue, which is located at about 10 Å from the sixth free coordination position of the reduced iron center II, becomes a ligand of the Fe^{3+} ion in the oxidized center II (*12*, *13*, *24*).

Protonation processes are essential for the reaction catalyzed by SOR, since two protons are required for the formation of H_2O_2. In this work, we have investigated the effect of pH on the spectral, redox, and kinetic properties of the active site of the SOR from *D. baarsii* in the absence and in the presence of $O_2^{\bullet-}$. The results led us to extend our initial previous studies (*17*, *18*) and to define precisely the nature of the two reaction intermediates in the catalytic cycle of SOR. The precise step of the catalytic cycle where protonation takes place was identified. These results are at variance with those recently reported by others. We propose a novel, complete scheme for a two-intermediate reaction of SOR with superoxide.

MATERIALS AND METHODS

Materials. For pulse radiolysis and γ-ray irradiation experiments, sodium formate and buffer salts were of the highest quality available (Prolabo Normatom or Merck Suprapure). Oxygen was delivered by ALPHA GAZ (purity higher than 99.99%); water was purified using an Elga Maxima system (resistivity 18.2 MΩ). KO_2 was from Merck. Anhydrous Me_2SO was from Aldrich. K_2IrCl_6 was from Strem Chemical Inc.

Overexpression and Purification of SORs. The gene encoding SOR from *D. vulgaris* Hildenborough was subcloned into the pMJ25 (*25*) vector as follows. First, an *Eag*I restriction site (underlined) was inserted downstream from the *Eco*RI site of pMJ25 vector by site-directed mutagenesis, using the primers 5′-GAG AGC GGC CGA TGC CCG AG-3′ and 5′-CTC GGG CAT CGG CCG CTC TC-3′. The DNA fragment from pJK15 (*25*), containing the *D. vulgaris* Hildenborough *sor* gene, was amplified by PCR using the primers 5′-AAA TTA CGG CCG ATG CCC AAC CAG TAC G-3′ and 5′-TAA AAT AAG CTT TTA GGC TTC GGC CTT CC-3′, containing an *Eag*I and a *Hind*III restriction sites (underlined), respectively. The amplified fragment was subcloned into the modified pMJ25 vector using *Hind*III and *Eag*I restriction sites. The resulting plasmid, pCW1, which placed the *D. vulgaris sor* gene under the control of

a *ptac* promoter, was transformed in *Escherichia coli* DH5α. The construct was verified by sequencing (GenomeExpress, France). The recombinant SOR from *D. vulgaris* Hildenborough was expressed from DH5α pCW1 in M9 minimum media, as described for the SOR from *D. baarsii* (*17*).

Recombinant SORs from *D. baarsii*, wild-type, E47A, and K48I mutated forms were expressed in *E. coli* as previously described (*17*). Proteins were purified by gel filtration on ACA54 followed by anion exchange chromatography on UnoQ6 (Bio-Rad) (*17*). At this stage, the three SOR proteins appeared to be homogeneous, as shown by SDS−PAGE analysis (15% acrylamide), and exhibited an $A_{280\ nm}/A_{503\ nm}$ ratio of 4.8−4.9. The *D. vulgaris* protein was purified using the same two-step protocol as for the *D. baarsii* enzyme. The protein was obtained homogeneous as shown by SDS−PAGE analysis (15% acrylamide) and exhibited an $A_{280\ nm}/A_{503\ nm}$ ratio of 4.8−4.9, as reported in ref *10*.

Full metalation of the two mononuclear iron sites was checked by atomic absorption spectroscopy. All the proteins were isolated with an oxidized center I ($\epsilon_{503\ nm} = 4400\ M^{-1}\ cm^{-1}$) and a fully reduced center II. Oxidation of center II was achieved by addition of a slight molar excess of K_2IrCl_6. Alternatively, in some cases, center II was oxidized by superoxide, by addition of KO_2 prepared in anhydrous Me_2SO, as reported in ref *3*. UV−visible absorption measurements were made on a Varian Cary 1 Bio spectrophotometer. EPR spectra were recorded on a Bruker ESP 300E spectrometer fitted with an Oxford Instruments ESR 900 helium flow cryostat.

pH Studies. The different buffers used to cover a 5.0 to 10.2 pH range were the following: pH 5.0 and 5.5, acetate buffer; pH 6.5, 7.0, and 7.5, phosphate buffer; pH 7.6, 8.1, and 8.5, Tris-HCl buffer; pH 9.1, 9.5, and 10.2, glycine-NaOH buffer.

Potentiometric Titrations. The redox titrations were carried out anaerobically at 22 °C in 50 mM of the different buffers used under an argon atmosphere, as described elsewhere (*26*). Optical measurements were performed with a Kontron 932 spectrophotometer equipped with a specially designed anaerobic sample cuvette containing 1.5 mL of 50 μM protein solution, in the presence of the following mediators at 3 μM each: ferrocene monocarboxylic acid (+530 mV), 1,4-benzoquinone (+280 mV), diethylaminodiethane (+240 mV), 2,5-dimethyl benzoquinone (+180 mV), phenazine methosulfate (+80 mV). The protein solution was first oxidized by addition of 10 mM K_2IrCl_6, and the reduction was conducted by stepwise additions of small quantities of 10−20 mM sodium dithionite in the same buffer. The redox potentials were measured with a combined Pt-Ag/AgCl/KCl (3 M) microelectrode and given in the text with respect to a standard hydrogen electrode. After each addition of sodium dithionite, the solution was left for 5 min so the thermodynamic equilibrium could be reached.

Pulse Radiolysis Experiments. Free radicals were generated by 200 ns pulses of 4.5 MeV electrons, from a linear accelerator located at the Curie Institute (*27*). The doses per pulse (5−15 Gy) were calibrated from the absorption of the thiocyanate radical $(SCN)_2^{\bullet-}$ obtained by radiolysis of thiocyanate ion solution in N_2O-saturated phosphate buffer ($[SCN^{\bullet-}] = 10^{-2}$ M, 10 mM phosphate, pH 7, $G(SCN)_2^{\bullet-} = 0.55\ \mu mol\ J^{-1}$, $\epsilon_{472\ nm} = 7580\ M^{-1}\ cm^{-1}$) (*28*). Superoxide radicals were generated in less than 1 μs by scavenging of radiolytically generated $HO^{\bullet}$ free radicals by 100 mM formate, in O_2 saturated solution as described (*29*). Samples to be irradiated were made up in 100 mM sodium formate complemented with 10 mM of the different buffers used, and saturated with pure O_2 by flushing over the surface of the solution with gentle shaking, thus avoiding direct bubbling in it. It lasted ca. 1 h for 1.5 mL of solution. Unless otherwise stated, the doses per pulse were ca. 5 Gy ($[O_2^{\bullet-}] \approx 3\ \mu M$). The $O_2^{\bullet-}$ concentration and self-decay were also assayed from its own absorbance at 271 nm ($\epsilon_{271\ nm} = 1400\ M^{-1}\ cm^{-1}$) and compared to literature data (*30*). The protein concentration was always between 70 and 150 μM. The reaction was followed spectrophotometrically between 450 and 750 nm, at 20 °C, in a 2-cm path length cuvette designed for pulse radiolysis experiments. The monochromator was calibrated using a laser which emits at 632.6 nm. Time-dependent difference absorbances were recorded on a Pro-92 Nicolet Instruments digital oscilloscope. Kinetics were always analyzed at different wavelengths. The traces could always be fitted according to a first-order kinetic law, using the Levenberg−Marquardt algorithm from KaleidaGraph (Synergy Software).

γ-ray Irradiations. γ-ray irradiations were carried out at 20 °C using a cobalt-60 source, at a dose rate of 18 Gy min^{-1}. The SOR proteins to be irradiated, 55 μM in plastic tubes fitted with septum inlet adapters, were made up in 10 mM Tris-HCl buffer pH 7.6, 100 mM sodium formate, 500 units/mL of catalase from *Aspergillus niger* and saturated with pure O_2 at room temperature, by passing O_2 over the surface of the solution for 1 h. The duration of irradiation was 5 min, to obtain a stoichiometric amount of $O_2^{\bullet-}$ relative to SOR. Immediately after irradiation, UV−visible spectra of the solution were recorded, in parallel with that of a nonirradiated solution kept under the same conditions. Completion of the oxidation of SOR by $O_2^{\bullet-}$ was checked with a sample solution irradiated for a longer time period and by addition of a stoichiometric amount of K_2IrCl_6.

RESULTS

pH Stability of SOR. The stability of the two iron centers of the wild-type, E47A and K48I SOR at different pHs was first determined by UV−visible absorption spectroscopy. In the three proteins, both the reduced and K_2IrCl_6 oxidized forms of the two iron centers were stable between pH 5.0 and 9.5, for at least 120-min incubation at room temperature (data not shown). However, center II was rapidly degraded above pH 9.5 (data not shown). At pH 10.2, the highest pH value investigated, the iron center II was not stable for over 10 min, hence precluding redox titration and pulse radiolysis above pH 9.5.

Spectroscopic Properties of SOR at Different pHs. The pH dependencies of the absorbance band of the K_2IrCl_6 oxidized center II of the wild-type, E47A, and K48I proteins are shown in Figure 1. In all cases, the absorbance spectrum of the oxidized center I was pH-insensitive (data not shown). Upon increasing the pH, the absorption band of center II exhibited a 84-nm blue shift from 644 to 560 nm in the three proteins. However, this shift occurred at higher pH for the wild-type protein (Figure 1A) than for the K48I (Figure 1B) and E47A (Figure 1C) mutants. For all proteins, this process was fully reversible with the pH (data not shown). A pH

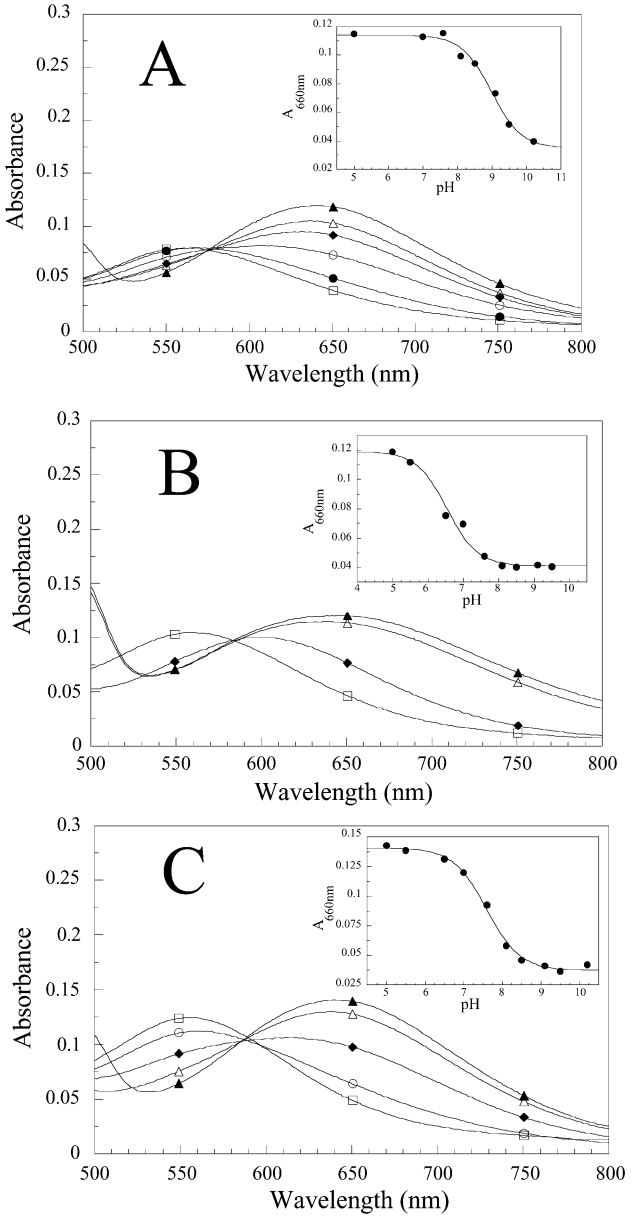

FIGURE 1: pH dependence of the light absorption spectra of wild-type SOR, E47A, and K48I SOR mutants. The enzymes (61.3 μM in 10 mM of the different buffers) were exposed to a slight excess of K_2IrCl_6, and the spectra were recorded immediately. (A) Wild-type enzyme at pH 5.0 (▲), pH 8.1 (△), pH 8.5 (◆), pH 9.1 (○), pH 9.5 (●), and pH 10.2 (□). (B) E47A mutant at pH 5.0 (▲), pH 5.5 (△), pH 7.0 (◆) and pH 8.5 (□). (C) K48I mutant at pH 5.5 (▲), pH 7.0 (△), pH 7.6 (◆), pH 8.1 (○) and pH 10.2 (□). The insets show the pH dependence of the absorbance at 660 nm. The titration curves fitted the equation expected from a single protonation process, $A_{660} = (A_{660max} + A_{660min} \times 10^{(pH-pK_a)})/(1 + 10^{(pH-pK_a)})$.

titration of this process was followed at 660 nm, where the 560 and 644 nm bands exhibit a maximum of absorbance change. The titration curve fitted the equation expected from a single protonation process (insets, Figure 1A−C) with pK_a values of 9.0 ± 0.1 for the wild-type protein, 6.7 ± 0.2 for the E47A and 7.6 ± 0.1 for the K48I protein (Figure 1 and Table 1).

This protonation process which likely occurs in the vicinity of center II can be observed also by EPR spectroscopy. In their oxidized state, centers I and II give low-temperature EPR lines in the same spectral region, around $g = 4.3$ (*3*, *10*). Because of the strong difference between the redox potential of the two centers (see below), the EPR signal of center II could be obtained by subtracting the EPR spectra of the as-prepared protein from that given by the K_2IrCl_6 oxidized protein. In the wild-type protein at pH 7.6, center II exhibits at 6 K a nearly isotropic line centered at $g = 4.3$ (Figure 2) characteristic of a high spin Fe^{3+} ion in a rhombic ligand field (*3*, *10*). At pH 10.2, a value higher than the pK_a measured by optical spectroscopy, the center II EPR spectrum becomes more complex, with a splitting of the positive peak and a broadening of the negative weak one, which indicates a change of the *g*-tensor rhombicity (Figure 2). Similar spectra were obtained for the E47A and K48I mutants, but at different pH values (5.0 and 7.6 for E47A, 6.0 and 8.5 for K48I, data not shown), below and above the pK_a determined by optical spectroscopy. This indicates that the same protonation process occurs in the wild-type and mutant proteins.

Table 1: pK_a Values of the Iron Center II of Wild-Type and Mutant Forms of *D. baarsii* SOR

SOR	absorbance transition[a]	potentiometric titration[b]
wt	9.0 ± 0.1	9.0
E47A	6.7 ± 0.2	6.6
K48I	7.6 ± 0.1	7.6

[a] From Figure 1. [b] From Figure 3C.

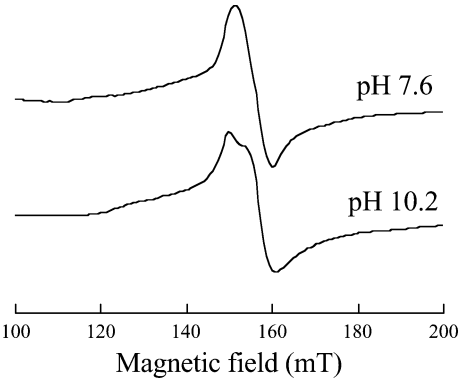

FIGURE 2: Influence of pH on the EPR signal of center II in the wild-type SOR. The signal shown results from spectral difference between the as-prepared and fully oxidized proteins. Conditions: temperature, 6 K; microwave power, 1 mW at 9.42 GHz; modulation amplitude, 1 mT at 100 kHz.

Redox Titration of SOR at Different pHs. Potentiometric titration of the wild-type, E47A, and K48I SORs were monitored by optical absorption spectroscopy in the pH 5.5−9.5 range. The iron centers were oxidized by addition of a stoichiometric amount of K_2IrCl_6, and the redox dependence of their absorption spectra was studied by successive addition of sodium dithionite. Dye mediators were carefully chosen to achieve redox equilibrium between the protein and the electrode in the range of potential investigated (+600 to −200 mV vs NHE) and to give as minor as possible spectral contribution in the 400−700 nm region. The reversibility of the redox process was checked by reoxidizing the fully reduced protein by addition of K_2IrCl_6 and was observed in all instances (data not shown). The redox potentials were determined from the absorbance variations recorded at 503 nm (where both centers I and II exhibit absorption in their oxidized state) and at 644 nm (where the absorption is almost exclusively due to the oxidized center II) (Figure 3A). All

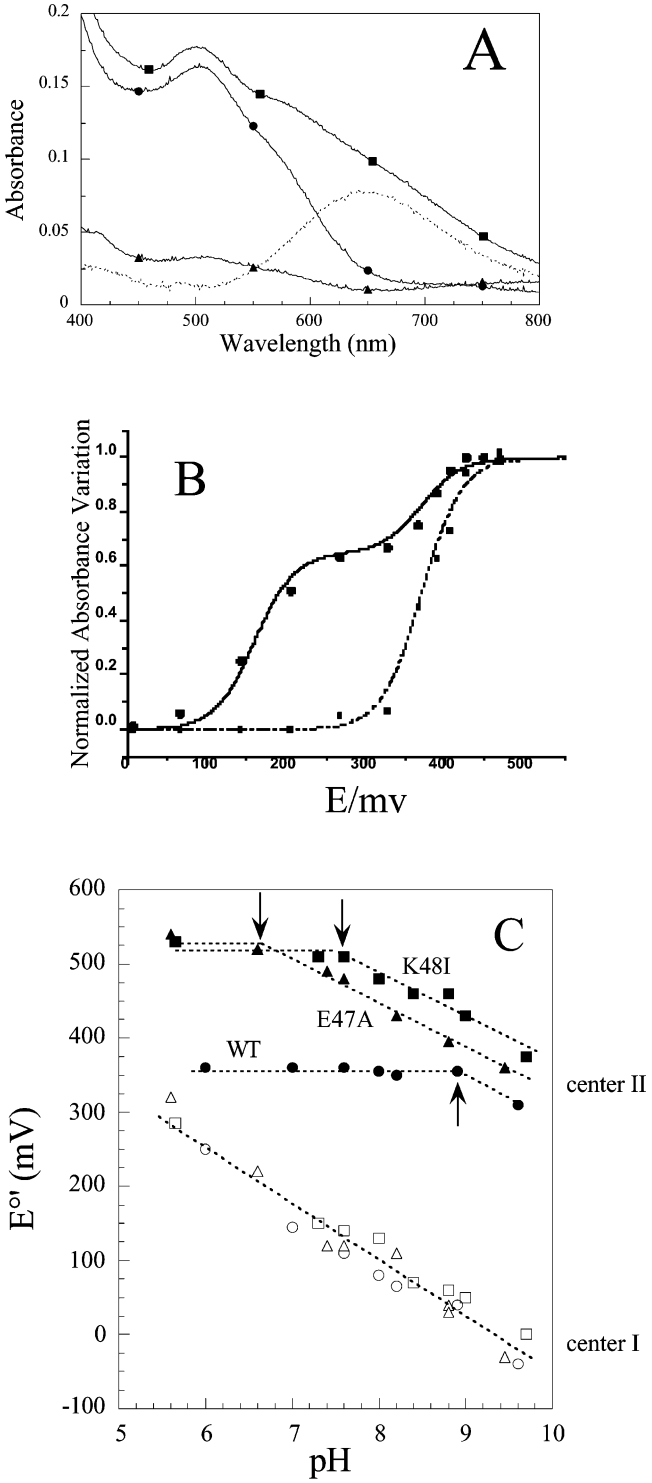

FIGURE 3: Redox properties of SOR. (A) Absorption spectrum of wild-type SOR in the as-prepared (●), fully oxidized (■), and fully reduced (▲) states. Dots are the difference spectrum between the oxidized and as prepared protein and represent the absorption spectrum of oxidized center II. (B) Reductive titration of the wild-type SOR at pH 7.0. Normalized variations of the absorbance at 503 nm (●) and 644 nm (■). The solid line corresponds to two independent one-electron Nernst plots centered at +370 and +160 mV and contributing to 35 and 65% of the total absorbance variation, respectively. The dashed line is a one-electron Nernst curve centered at +370 mV. (C) pH-dependence of the redox potential of centers I (open symbols) and II (full symbols) in wild-type (○, ●), E47A (△, ▲), and K48I (□, ■) SORs.

titration curves at 503 nm fitted a two-step one-electron redox process, whereas the titration curves at 644 nm fitted a one-electron-transfer mechanism (Figure 3B). Identical values were obtained for the redox potential of center II from the 503 and 644 nm titration curves.

As shown in Figure 3C, the redox potential of the wild-type SOR center II was pH-independent from pH 6.0 to pH 9.0, with a midpoint potential value of +350 mV vs NHE. This value is slightly more positive than the value reported for other SOR iron centers II (*8*−*10*, *13*, *14*). For both E47A and K48I SOR mutants at acidic pH, the redox potential of center II was about 170 mV above that of the wild-type protein, with a midpoint potential of +520 mV vs NHE at pH 5.5. However, upon increasing the pH, the redox potential of both mutants turned out to be pH-dependent, with a 59 ± 4 mV slope per pH unit (Figure 3C). pH values associated with the transition for the pH dependence of the redox potential were estimated at 6.6 for the E47A mutant and 7.6 for the K48I mutant (Figure 3C, Table 1). A similar pH dependence for the redox potential of the wild-type protein also stands at pH values above 9.0 (Figure 3C, Table 1). However, because of the instability of the iron center II at basic pH, the redox potentials could not be determined accurately above pH 9.5.

As shown in Figure 3C, the redox potentials of center I for the wild-type E47A and K48I mutant proteins decreased in parallel by increasing the pH with a slope of 66±6 mV per pH unit. This indicates that the reduction of center I is coupled with a one-proton transfer in the pH range 5.5−9.5, with a pK_a value below 5.5.

Pulse Radiolysis of Wild-Type SOR at Different pHs. To study the role of protonation processes during the reaction of SOR with $O_2^{\bullet-}$, we carried out pulse radiolysis experiments over the pH range 5.0−9.5. The experimental conditions were similar to those described in our previous study (*17*): the wild-type and mutant SOR proteins were present in large excess with regard to superoxide ([SOR] = 100 μM, [$O_2^{\bullet-}$] = 3 μM).

Figure 4 shows representative kinetic traces, recorded at 575 and 625 nm, of the reaction of SOR wild-type with $O_2^{\bullet-}$, at three pH values. Similar kinetic experiments were repeated at pH 5.0, 5.5, 6.5, 7.0, 7.6, 8.1, 8.5, 9.1, 9.5 and at different wavelengths, every 5 to 10 nm between 500 and 700 nm (data not shown). The traces observed in the wavelength region 500−615 nm always showed a fast increase followed by a decrease of absorbance. Conversely, around 625 nm the absorbance increased first and remained constant or varied slightly with time (Figure 4). The final values of the first and second transformations were reached at the same time at all wavelengths, showing that the bulk reaction consisted of two steps in sequence.

For each pH value, the rate constants k_1 and k_2 for the formation of the first and the second intermediate, respectively, were determined (Table 2). At all the different wavelengths investigated, the rate constants associated to the formation of each intermediate were identical and were averaged thereof. The formation of the first intermediate was not affected by the pH and exhibited a maximum at ca. 50−100 μs after the pulse (Figure 4). On the other hand, the rate of the formation of the second intermediate is strongly decreased as the pH of the reaction rises. For example, at pH 5.5, the formation of the second intermediate was over 150 μs after the pulse (Figure 4) and its absorbance

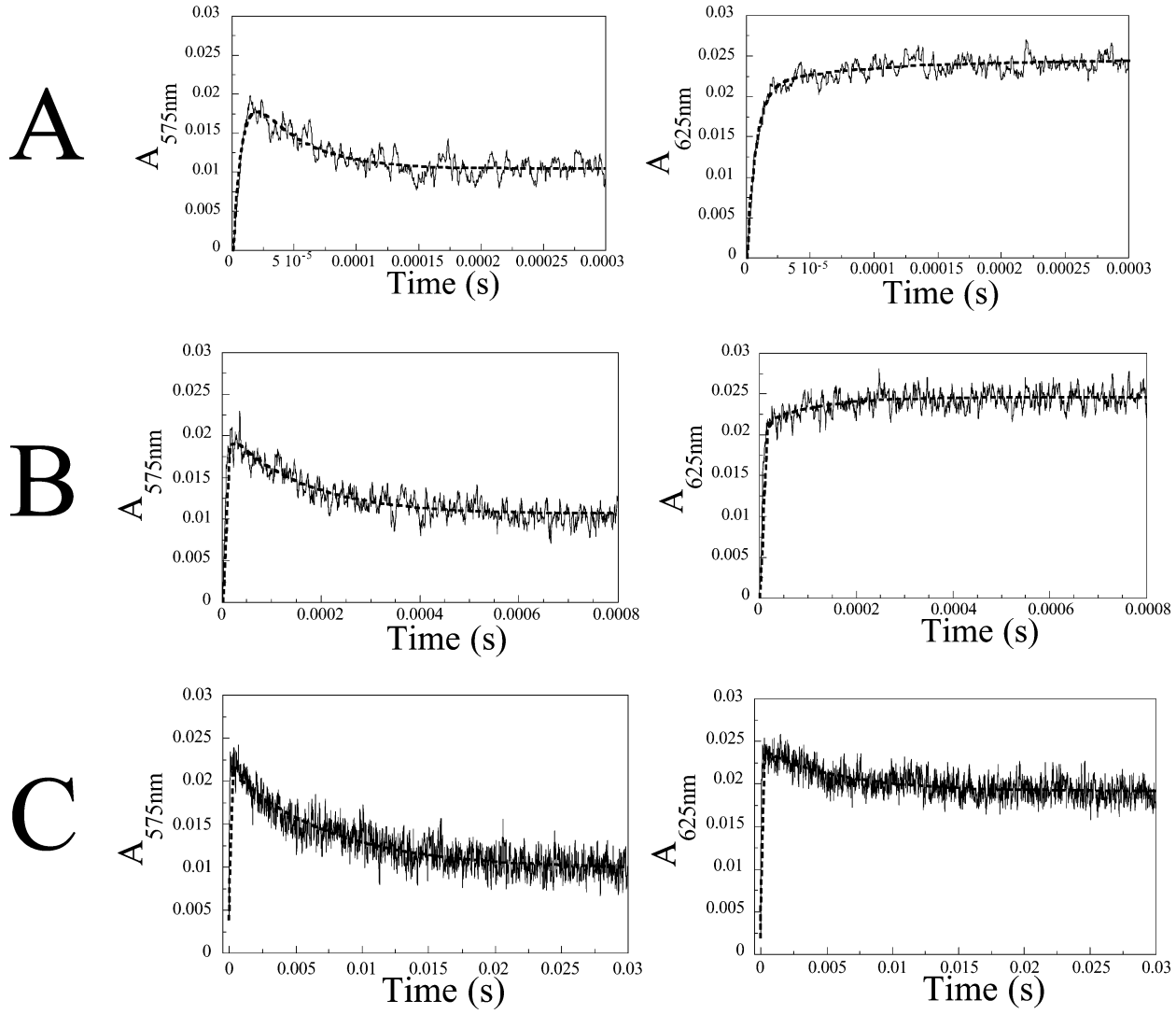

FIGURE 4: Digital oscilloscope recordings showing the reaction of wild-type SOR (100 μM) with $O_2^{\bullet-}$ (3 μM) generated by pulse radiolysis at pH 5.5 (A), pH 7.0 (B), and pH 8.1 (C). Electron pulses were 5 ± 1 Gy. The observation wavelength was fixed at 575 (left) and 625 nm (right). The dashed lines were calculated for best fit to a biexponential model.

Table 2: Summary of the pH-Dependent Rate Constants, k_1 and k_2 for the Two Intermediates Formed during the Reaction of Various SORs with $O_2^{\bullet-}$ [a]

	k_1 (M^{-1} s^{-1})			k_2 (s^{-1})		
	D. baarsii			*D. baarsii*		
pH	wt (× 10^{-9})	E47A (× 10^{-9})	K48I (× 10^{-7})	wt	E47A	K48I
5.0	1.4 ± 0.2	1.6 ± 0.2	6.5 ± 0.2	140000 ± 20000	160000 ± 20000	nd[b]
5.5	0.9 ± 0.1	nd	nd	52400 ± 1500	19400 ± 7000	nd
6.5	1.5 ± 0.1	1.4 ± 0.1	6.1 ± 0.6	7570 ± 1140	13900 ± 2000	nd
7.0	1.3 ± 0.1	nd	6.1 ± 0.5	4280 ± 300	8000 ± 2000	1630 ± 140
7.6	1.1 ± 0.3	1.2 ± 0.2	4.2 ± 0.5	550 ± 50	440 ± 50	300 ± 30
8.1	nd	nd	4.3 ± 0.8	nd	nd	295 ± 75
8.5	nd	1.4 ± 0.1	4.7 ± 0.1	150 ± 30	200 ± 80	153 ± 13
9.1	1.3 ± 0.3	nd	nd	nd	153 ± 8	85 ± 17
9.5	nd	nd	nd	49 ± 7	nd	nd
	D. vulgaris Hildenborough			*D. vulgaris Hildenborough*		
7.6	8.0 ± 0.5 × 10^8			425 ± 20		

[a] The rate constants were determined from the time courses of absorbance changes at different wavelengths between 550 and 650 nm. Each value represents the average over at least five different measurements. [b] Not determined.

value remained stable for up to 30 ms (data not shown). At pH 8.1, its formation went to completion after ca. 25 ms (Figure 4).

As shown in Figure 5A, k_1 is constant over the pH range 5.0−9.5. On the other hand, as shown in Figure 5B, k_2 depends on pH in such a way that its logarithm exhibits a linear relationship with the H^+ concentration: $\log k_2 = \log k_0 - (0.80 \pm 0.05)$pH, where k_0 is the limit of the rate constant when the pH approaches zero and was calculated to be $(1.4 \pm 0.7) \times 10^9$ M^{-1} s^{-1}.

Table 3: Extinction Coefficients of the Intermediates[a] and Final Species[b] Formed during the Reaction of Wild-Type and Mutated SORs from *D. baarsii* with Superoxide, at Different pHs

SOR	first intermediate (M^{-1} cm^{-1})	second intermediate (M^{-1} cm^{-1})	final species Fe^{3+} (M^{-1} cm^{-1})	
			deprotonated (560 nm)	protonated (644 nm)
wt	$\epsilon_{605\ pH\ 7.6} = 2840 \pm 100$ $\epsilon_{605\ pH\ 9.1} = 3030 \pm 230$	$\epsilon_{625\ pH\ 7.6} = 2990 \pm 120$ $\epsilon_{625\ pH\ 5.0} = 3070 \pm 160$	$\epsilon > 1300$[c]	$\epsilon = 1900$
E47A	$\epsilon_{595\ pH\ 7.6} = 2750 \pm 80$ $\epsilon_{595\ pH\ 8.5} = 2660 \pm 290$	$\epsilon_{625\ pH\ 7.6} = 2870 \pm 210$ $\epsilon_{625\ pH\ 5.0} = 3370 \pm 150$	$\epsilon = 1600$	$\epsilon = 1900$
K48I	$\epsilon_{595\ pH\ 7.6} = 1960 \pm 80$ $\epsilon_{595\ pH\ 8.5} = 2230 \pm 210$	$\epsilon_{625\ pH\ 7.6} = 2430 \pm 180$ $\epsilon_{625\ pH\ 5.0} = 3170 \pm 190$	$\epsilon = 1900$	$\epsilon = 2300$

[a] Measured by pulse radiolysis. [b] Iron center II oxidized with a slight excess of K_2IrCl_6. [c] Full deprotonation occurs above pH 10.

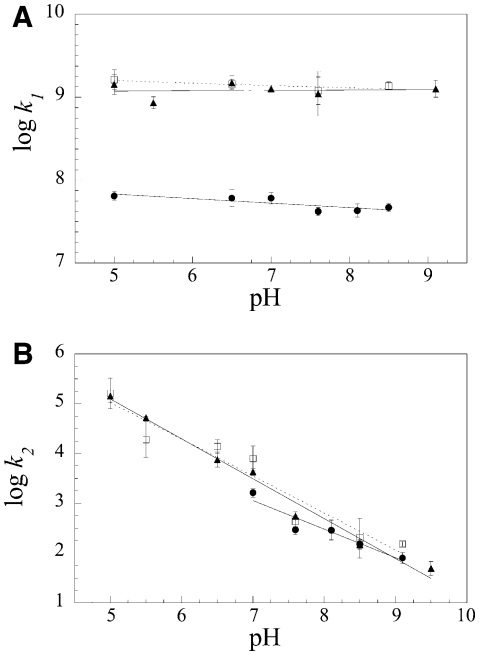

FIGURE 5: pH dependence of the logarithm of the rate constants k_1 (A) and k_2 (B) for the reaction of wild-type SOR (▲), E47A mutant (□), and K48I mutant (●) with $O_2^{\bullet-}$. k_1 did not vary significantly with pH. k_2 values were fitted to a linear equation, $\log k_2 = \log k_O - \alpha pH$. Found $\alpha = 0.80 \pm 0.05$, $k_O = 1.4 \pm 0.7 \times 10^9$ M^{-1} s^{-1} for the wild-type SOR; $\alpha = 0.75 \pm 0.10$, $k_O = 0.5 \pm 1.0 \times 10^9$ M^{-1} s^{-1} for the E47A mutant; $\alpha = 0.62 \pm 0.10$, $k_O = 0.3 \pm 0.6 \times 10^8$ M^{-1} s^{-1} for the K48I mutant.

The spectra of both intermediates were reconstructed at various pHs, using the absorbance values measured at different wavelengths, taken at their maxima. The time corresponding to these maxima did not vary with the wavelength. Figure 6A shows spectra for the first intermediate reconstructed at pH 7.6 and 9.1 and for the second one at pH 7.6 and 5.0. Reconstituted spectra at other pHs did not differ substantially (data not shown). Spectra of both intermediates did not change with pH. The first intermediate exhibits a broad absorption band centered around 605 nm, whereas the second one exhibits a sharp absorption band centered at 625 nm. The appearance of this 625 nm band was specific of the presence of reduced SOR and not associated with instrumentation or photodetection defects. Indeed, pulse radiolysis experiments carried out in the same conditions but in the absence of SOR or with the fully oxidized SOR gave no variation of absorbance up to 30 ms at 625 nm, and at all wavelengths investigated between 500 and 700 nm (data not shown).

The spectra of these two intermediates are very similar to those reported in our previous studies carried out at pH 7.6 (*17*). The spectrum of the second intermediate is clearly different from that of the final reaction species, the oxidized iron center II (Figure 6A). This was confirmed by γ-ray irradiation experiments, carried out under the same experimental conditions as pulse radiolysis to allow oxidation of SOR by stoichiometric amounts of superoxide anion (Figure 6A). Catalase was added in catalytic concentration to remove hydrogen peroxide. UV−visible spectra obtained after γ-ray irradiation are characteristic of the fully oxidized iron center II. Moreover, the formation of oxidized center II, determined from its ϵ value at 644 nm (1.9 mM^{-1} cm^{-1}), corresponds to the radiolytic yield for the formation of superoxide, in agreement with a stoichiometric reaction of $O_2^{\bullet-}$ with SOR.

The SOR from *D. vulgaris* Hildenborough, which was reported by other groups to operate with a single reaction intermediate during its turnover (*9*, *16*, *20*), was reacted with $O_2^{\bullet-}$ in pulse radiolysis experiments. The *D. vulgaris* enzyme gave the same reaction kinetics as the SOR from *D. baarsii* (data not shown and Table 2), with almost identical absorption spectra for the two detected reaction intermediates (Figure 6B). This is consistent with the formation of two reaction intermediates during the reaction of the *D. vulgaris* Hildenborough enzyme with $O_2^{\bullet-}$, and with the same reaction mechanism as the enzyme from *D. baarsii*.

To obtain accurate values of the extinction coefficient for the two intermediates of *D. baarsii* SOR at different pHs, absorbances at 605 or 625 nm were measured at their peak values in the presence of various concentrations of $O_2^{\bullet-}$. The radiation dose was varied from 6.0 to 13.5 Gy, yielding concentrations of $O_2^{\bullet-}$ from 4 to 8.5 μM at constant SOR concentration (100 μM) (Figure 6A). Peak absorbances were proportional to the $O_2^{\bullet-}$ concentration, indicating that Beer−Lambert's law was followed and that the reaction of SOR with $O_2^{\bullet-}$ was quantitative. As shown in Table 3, both intermediates exhibit molar extinction coefficient values of 2900−3000 M^{-1} cm^{-1}, which do not significantly vary with the pH. The extinction coefficient at 625 nm for the second intermediate is 60% higher than that of the final product of the reaction, oxidized iron center II (1900 M^{-1} cm^{-1} in the 625−645 nm region).

Pulse Radiolysis on SOR E47A and K48I Mutant Forms at Different pH. Pulse radiolysis experiments were carried out in the same way as above at different pH values with the E47A and K48I SOR mutants. As for the wild-type protein, both mutants gave traces that fit a biexponential process, corresponding to the formation of two reaction intermediates. For a given pH value, at all the different

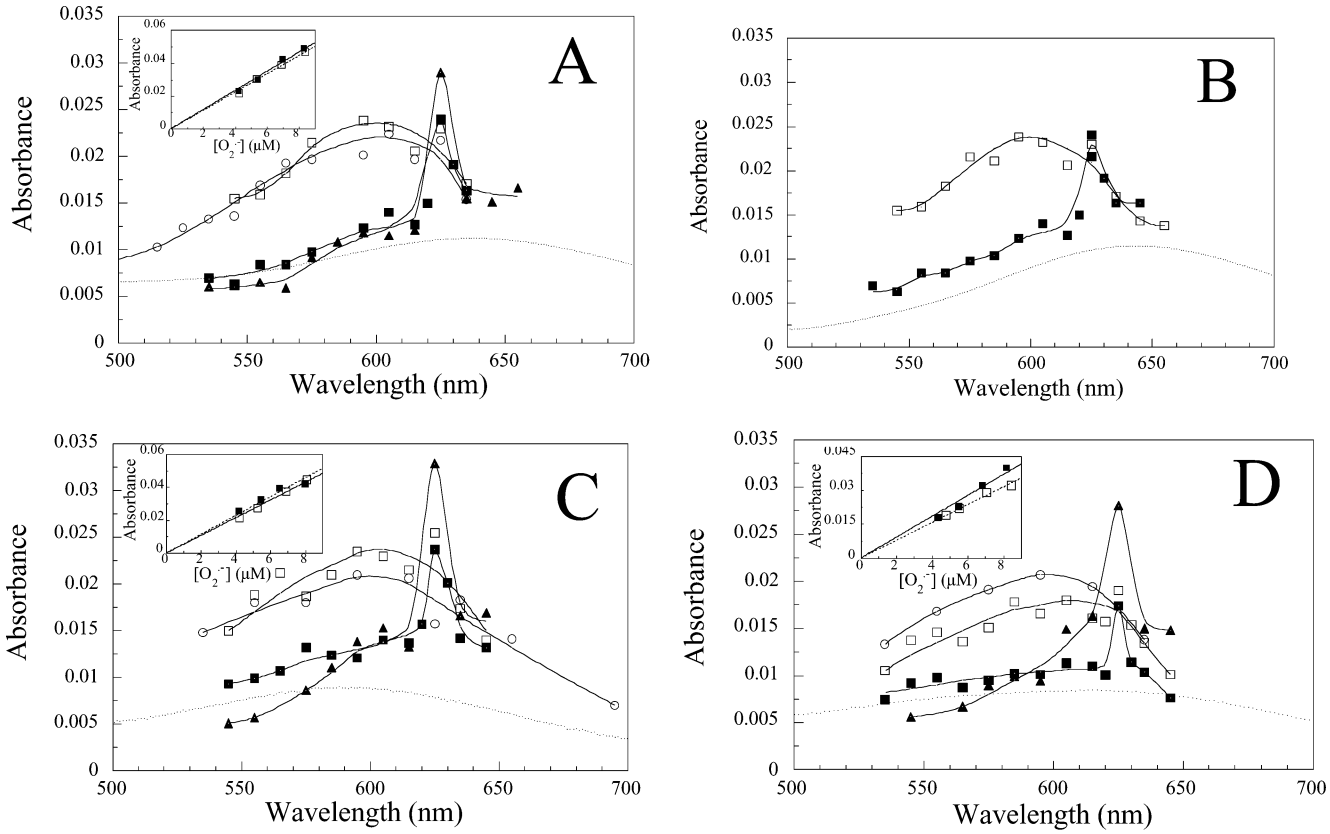

FIGURE 6: Transient absorption spectra (in a 2-cm path-length cuvette) formed upon reaction of wild-type and mutants SORs (100 μM) with $O_2^{\bullet-}$ (3 μM) generated by pulse radiolysis at different pHs. Open and closed symbols correspond to the reconstituted spectra of the first and second reaction intermediates, respectively. (A) Wild-type SOR from *D. baarsii*. (○) pH 9.1, 1 ms after the pulse. (□) pH 7.6, 100 μs after the pulse. (■) pH 7.6, 10 ms after the pulse. (▲) pH 5.0, 100 μs after the pulse. (B) Wild-type SOR from *D. vulgaris* Hildenborough. (□) pH 7.6, 100 μs after the pulse. (■) pH 7.6, 10 ms after the pulse. (C) E47A SOR mutant from *D. baarsii*. (○) pH 8.5, 100 μs after the pulse. (□) pH 7.6, 100 μs after the pulse. (■) pH 7.6, 10 ms after the pulse. (▲) pH 5.0, 100 μs after the pulse. (D) K48I SOR mutant from *D. baarsii*. (○) pH 8.5, 1.5 ms after the pulse. (□) pH 7.6, 1 ms after the pulse. (■) pH 7.6, 10 ms after the pulse. (▲) pH 5.0, 1 ms after the pulse. The dotted lines show the absorption spectrum of iron center II (3 μM, pH 7.6) of each SOR variant after complete oxidation by $O_2^{\bullet-}$ generated by γ-ray irradiation in the presence of a catalytic amount of catalase, or by reaction with a slight excess of K_2IrCl_6. The inserts show the maximal absorbances for the first (□, 605 nm) and second reaction intermediate (■, 625 nm) as a function of increasing amounts of $O_2^{\bullet-}$ generated by pulse radiolysis (6.0−13.5 Gy, pH 7.6). The extinction coefficients calculated from these curves are given in Table 3.

wavelengths investigated, the rate constants associated with the formation of each intermediate were found to be identical (Table 2).

The E47A mutation, which was previously shown to have no effect on the k_1 and k_2 values at pH 7.6 (*17*), yielded the same pH independence for k_1 (Figure 5A) and the same pH dependence for k_2 (Figure 5B) as the wild-type protein. In the pH range 5.0−9.5, we found $\log k_{2\ \mathrm{E47A}} = \log k_0 - (0.75 \pm 0.10)$ pH, with $k_0 = 0.5 \pm 1.0 \times 10^9\ \mathrm{M^{-1}\ s^{-1}}$ (Figure 5B and Table 2).

The K48I mutation, which at pH 7.6 was previously shown to decrease k_1 by a factor of 30 (*17*), showed no significant pH dependency of its k_1 values in the 5.0−8.5 pH range (Figure 5A). k_2 varied with pH, although the variation was less pronounced than for the wild-type and E47A proteins, with $\log k_{2\ \mathrm{K48I}} = \log k_0 - (0.62 \pm 0.10)$ pH, and $k_0 = 0.3 \pm 0.6 \times 10^8\ \mathrm{M^{-1}\ s^{-1}}$ (Figure 5B and Table 2). It should be noted that for the K48I mutant, the k_2 value could not be determined below pH 7.0, because the rate constant for the formation of the first intermediate was 30 times as low as for the wild-type and E47A proteins, and this became the limiting step.

Reconstituted spectra for the two intermediates in the case of the E47A mutant are very similar to those of the wild-type protein. Similarly, the shape of both spectra were unaffected by the pH (Figure 6C). The extinction coefficient values obtained by varying the radiolysis dose, at 595 and 625 nm for the first and the second intermediates, respectively, are very close to those determined for the wild-type protein, except for the extinction coefficient of the second intermediate, which seems to be significantly increased at acidic pH (Figure 6C and Table 3). Once again, the spectrum of the second intermediate clearly differs from that of the oxidized iron center II (Figure 6C).

Reconstituted spectra for the two intermediates in the case of the K48I mutant give also qualitatively similar results to those of the wild-type and E47A proteins (Figure 6D). In our previous work (*17*), we reported a spectrum for the second intermediate at pH 7.6 different from the one presented here. Indeed, the sharp band centered at 625 nm might be missed if measurements at wavelengths 620, 625, and 630 nm were not done. The shape of both spectra was unaffected by the pH (Figure 6D). However, except at pH 5.0 for the second intermediate, the extinction coefficient

Scheme 1

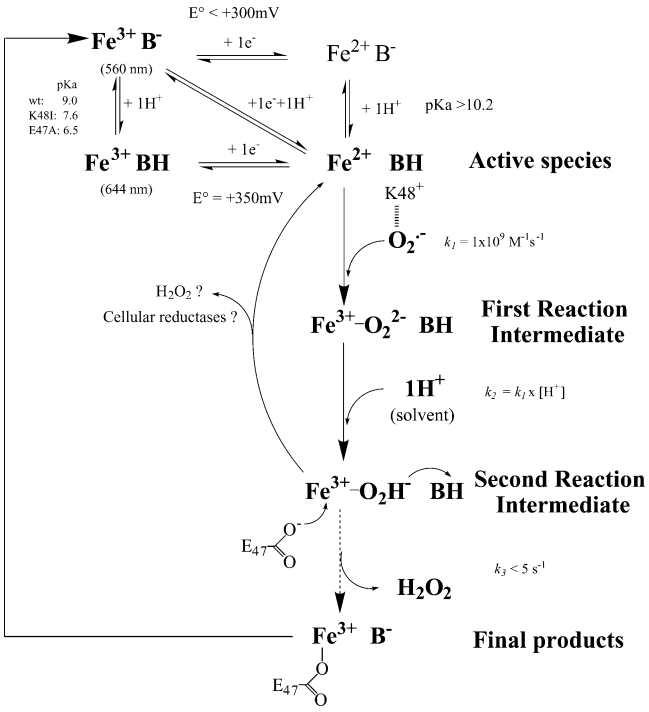

for both intermediates are significantly lower than for the wild-type protein (Table 3).

DISCUSSION

In this work, we have investigated the protonation processes that take place during the reaction of *D. baarsii* SOR with $O_2^{\bullet-}$. As two protons are required for the formation of H_2O_2, proton transfer is an essential step of catalysis. For this reason, the effect of pH on the reaction kinetics and the redox potential of the SOR active site were investigated in detail. Wild-type, E47A, and K48I SOR mutants were studied in parallel, and the role of the E47 and K48 residues in catalysis were specified. The results allow us to propose the reaction pathway described in Scheme 1. It completes our previous studies of the reaction mechanism (*17*).

Support for the Existence of Two Reaction Intermediates. Conflicting results on the catalytic mechanism of SOR have been reported in the literature, pointing out the presence of a single reaction intermediate only, in particular for the SOR from *D. vulgaris* Hildenborough (*9*, *16*, *20*). This is intriguing since this enzyme exhibits 70% sequence homology with the *D. baarsii* protein. According to the authors, the single reaction intermediate, with an absorption spectrum similar to that of our first reaction intermediate,undergoes direct protonation to give the final products of the reaction, namely, the oxidized center II and H_2O_2 (*20*). Our experimental data provide several lines of evidence in support of the existence of a second reaction intermediate during the catalytic cycle of SOR with $O_2^{\bullet-}$.

(i) The spectrum of this second intermediate shows a characteristic sharp peak at 625 nm and is reproducibly observed in all preparations of SOR at all the different pHs studied. It is specific of the presence of both the enzyme and $O_2^{\bullet-}$ in the cuvette. Its extinction coefficient at 625 nm was precisely determined at pH 7.6 and appeared to be 40% higher than that of oxidized center II (Table 3). In addition, in our hands the SOR from *D. vulgaris* Hildenborough also elicited two reaction intermediates when reacted with $O_2^{\bullet-}$, with absorption spectra similar to those of the *D. baarsii* enzyme. This is consistent with the high sequence homologies between these two enzymes.

(ii) The second intermediate is not the end product of the reaction under pulse radiolysis conditions. This was confirmed by γ-ray irradiation experiments, which are more appropriate for investigation of the final product of the reaction. In addition, the spectrum of the final product, which occurs after at least 50−100 ms of the reaction time with $O_2^{\bullet-}$, is identical to that of the oxidized form of SOR obtained after treatment with K_2IrCl_6, xanthine oxidase, or KO_2 (*3*).

(iii) Resonance Raman experiments have previously shown that the E47A mutation in *D. baarsii* SOR allows a strong stabilization of an iron(III)-peroxo intermediate, implying that E47 is involved in H_2O_2 release from the peroxo intermediate (*21*). This role for the E47 residue is in agreement with the observation that E47 becomes a ligand of the final product of the reaction, the oxidized active center of SOR (*12*, *24*). From these data, one would expect a large decrease of the rate constant of peroxide release in the E47A SOR mutant. However, no kinetic effects associated with the E47A mutation were observed by pulse radiolysis. Once again, this is consistent with the fact that the last step of the reaction, corresponding to peroxide release, is not observed during pulse radiolysis studies.

Proton Transfer Is a Determinant of the Second Step of the Reaction. The formation of the first reaction intermediate was described at pH 7.6 as a bimolecular reaction of SOR with $O_2^{\bullet-}$ (*17*). The present data show that its formation does not involve proton transfer as a rate-limiting step, since the rate constant k_1 does not vary between pH 5.0 and pH 9.5. This suggests that the first reaction intermediate is an Fe^{3+}-peroxo species, assuming an inner-sphere mechanism for the reaction of SOR with $O_2^{\bullet-}$ and that the SOR active site was shown to stabilize transiently such species (*21*) (Scheme 1).

On the other hand, the rate constant k_2 for the formation of the second reaction intermediate is proportional to the H^+ concentration in solution. This points to proton transfer as the rate-limiting step and corroborates an Fe^{3+}-hydroperoxo species structure for the second reaction intermediate (Scheme 1). However, the plot of k_2 versus pH is not sigmoidal. This suggests that the proton arises directly from the solvent, which is in line with the solvent exposed active site of SOR (*5*, *12*). Then, no specific base in the active site is apparently required for this protonation step.

At pH 5.0 (the lowest pH value investigated here), a significant amount of $HO_2^{\bullet}$ (pK_a 4.8) is present in solution after the pulse. Nevertheless, no measurable pH effect was observed on the rate constant k_1. It indicates that $O_2^{\bullet-}$ and $HO_2^{\bullet}$ react equally well with SOR. In this pH region, the reaction ends directly in the second reaction intermediate, the Fe^{3+}-hydroperoxo species, without evidence for a transient accumulation of the first reaction intermediate.

Presence and Role of a Base in the Active Site. The presence of a base in close proximity to the iron center II is strongly supported by our experimental data. Deprotonation of this base results in modifications of the EPR spectra and in a 84-nm blue shift of the absorbance maximum of the oxidized active site, from 560 to 644 nm. Moreover, above a certain pH value, the redox potential of the iron center II

turns out to depend on pH, indicating the necessity for a one-proton transfer associated with reduction of the iron center. The pK_a value measured from potentiometric titration was identical to that determined from the blue-shift transition of the absorption spectra (Table 1), suggesting that a single base (B^- in Scheme 1) is sufficient to modulate the redox and spectral properties of the active site.

Nevertheless, the catalytical function of this base during the reaction of SOR with superoxide remains unclear. Its protonated form (BH in Scheme 1) in the reduced SOR is clearly not involved in the protonation process of the first intermediate during the reaction with superoxide. This is clear from the pH dependence of the rate constant k_2 for the formation of the second intermediate, as discussed above. In addition, whereas deprotonation of this base has a strong effect on the spectrum of the oxidized center II, no modification of the spectra of both reaction intermediates was observed in the 5−9.5 pH range. Since in these spectra, in addition to a peroxo-to-Fe^{3+} charge-transfer band, one would expect a strong contribution of the absorption band of the oxidized center II (Cys-to-Fe^{3+} charge-transfer band) (*13*), this again suggests that this base remains protonated in these conditions.

We propose that BH might be involved in the last step of the reaction and could provide a second proton at the stage of the iron(III)-hydroperoxide to produce H_2O_2 (Scheme 1).

The nature of this base responsible for the acidic−basic properties of the iron center II is not known yet. It is not the side chain of E47 or of K48. However, both residues interact with it, as judged from the effect of the mutations E47A and K48I on the pK_a value (Table 1). The large pH effect on the light absorption spectra and changes of the *g*-tensor rhombicity suggest that this base is located in the coordination sphere of the iron center II. In the case of the SOR from *P. furiosus* a similar blue-shift transition has been described between pH 7.6 and 10. Resonance Raman studies on the *P. furiosus* enzyme at pH values above and below the blue-shift transition did not reveal any spectral changes, including in the low-frequency region associated with the N(His) to iron (III) vibration mode (*31*). This suggests that no modification of the histidine coordinations occurs during this process and that there is no protonation at the level of the (His)N involved in the iron coordination. However, we might consider that the protonation process concerns one of the (His)N−H not involved in the iron coordination. This remains to be clearly established.

The Redox Potential of the Iron Center II Is Not a Determinant of the Reaction with Superoxide in the Region 350−550 mV vs ENH. Both the E47A and K48I mutations increase the redox potential of the iron center II (+170 mV at pH 7.6), with a pH dependence above pH 6. These changes do not affect the reactivity of the active site with $O_2^{\bullet-}$. In fact, the second-order rate constant of the reaction of SOR with $O_2^{\bullet-}$ did not vary significantly with pH above 6, whereas the redox potential of both mutant decreased by 60 mV per pH unit, from +520 (pH 6) to +300 mV (pH 9.5). Altogether, these data suggest that the value of the standard redox potential of the various SORs, close to +300 mV, is not determinant for an efficient reactivity with $O_2^{\bullet-}$. In all cases, this potential remains well below that of the $O_2^{\bullet-}/H_2O_2$ couple, ($E'_0 \approx +900$ mV), which makes the reaction still very thermodynamically favorable.

Role of the E47 and K48 Amino Acid Residues in Catalysis. Although E47 and K48 are the charged residues closest to the sixth free coordination position of the iron atom, our data show that they are not involved in proton donation during catalysis. Indeed, the E47A and K48I mutations had no effect on the pH dependence profile for the formation of the second intermediate. In contrast, the remarkable effect of the K48I mutation on the value of the rate constant k_1 suggests an important role for K48 in electrostatic attraction of the superoxide anion into the active site.

Under our experimental conditions, H_2O_2 release from the second reaction intermediate could not be observed kinetically within the 30−50 ms of the reaction time with $O_2^{\bullet-}$, suggesting a rate constant below 5 s^{-1}. This step might even be slower than that of electron transfer from reduced rubredoxin (*6*) or NAD(P)H cellular reductases (Lombard et col., personal communication) to the oxidized form of SOR (rate constant of about 10^6 M^{-1} s^{-1}) (Scheme 1). It could be then likely that the cellular reductases reduce directly the iron(III)-hydroperoxo species into the reduced iron center II and H_2O_2 (Scheme 1). In that case, the Fe^{3+} form with the E47 as the sixth ligand would be outside the catalytical cycle of SOR. E47 could be involved in H_2O_2 release from the peroxo intermediate in the absence of functional cellular reductases.

ACKNOWLEDGMENT

We thank Jean-Luc Ravanat for kindly providing an access to a cobalt-60 source for γ-ray irradiations. We acknowledge Gerard Baldacchino for discussions and pulse radiolysis experiments. We are grateful to Marc Fontecave for constant support in this work.

REFERENCES

1. Sies, H. (1986) *Angew. Chem., Int. Ed. Engl. 25*, 1058−1071.
2. Fridovich, I. (1995) *Annu. Rev. Biochem. 64*, 97−112.
3. Lombard, M., Fontecave, M., Touati, D., and Nivière, V. (2000) *J. Biol. Chem. 275*, 115−121.
4. Jenney, F. E., Jr., Verhagen, M. F. J. M., Cui, X., and Adams, M. W. W. (1999) *Science 286*, 306−309.
5. Coelho, A. V., Matias, P., Fülöp, V., Thompson, A., Gonzalez, A., and Carrondo, M. A. J. (1997) *J. Biol. Inorg. Chem. 2*, 680−689.
6. Emerson, J. P., Coulter, E. D., Phillips, R. S., and Kurtz, D. M., Jr. (2003) *J. Biol. Chem. 278*, 39662−39668.
7. Lombard, M., Touati, D., Fontecave, M., and Nivière, V. (2000) *J. Biol. Chem. 275*, 27021−27026.
8. Jovanovic, T., Ascenso, C., Hazlett, K. R. O., Sikkink, R., Krebs, C., Litwiller, R., Benson, L. M., Moura, I., Moura, J. J. G., Radolf, J. D., Huynh, B. H., Naylor, S., and Rusnak, F. (2000) *J. Biol. Chem. 275*, 28439−28448.
9. Emerson, J. P., Cabelli, D. E., and Kurtz, D. M., Jr. (2003) *Proc. Natl. Acad. Sci. U.S.A. 100*, 3802−3807.
10. Tavares, P., Ravi, N., Moura, J. J. G., LeGall, J., Huang, Y. H., Crouse, B. R., Johnson, M. K., Huynh, B. H., and Moura, I. (1994) *J. Biol. Chem. 269*, 10504−10510.
11. Verhagen, M. F. J. M., Voorhorst, W. G. B., Kolkman, J. A., Wolbert, R. B. G., and Hagen, W. R. (1993) *FEBS Lett. 336*, 13−18.
12. Yeh, A. P., Hu, Y., Jenney, F. E., Jr., Adams, M. W. W., and Rees, D. C. (2000) *Biochemistry 39*, 2499−2508.
13. Clay, M. D., Jenney, F. E., Jr., Hagedoorn, P. L., George, G. N., Adams, M. W. W., and Johnson, M. K. (2002) *J. Am. Chem. Soc. 124*, 788−805.
14. Abreu, I. A., Saraiva, L. M., Carita, J., Huber, H., Stetter, K. O., Cabelli, D. E., and Teixeira, M. (2000) *Mol. Microbiol. 38*, 322−334.
15. Silva, G., LeGall, J., Xavier, A. V., Teixeira, M., and Rodrigues-Pousada, C. (2001) *J. Bacteriol. 183*, 4413−4420.

16. Coulter, E. D., Emerson, J. P., Kurtz, D. M., Jr., and Cabelli, D. E. (2000) *J. Am. Chem. Soc. 122*, 11555−11556.
17. Lombard, M., Houée-Levin, C., Touati, D., Fontecave, M., and Nivière, V. (2001) *Biochemistry 40*, 5032−5040.
18. Nivière, V., Lombard, M., Fontecave, M., and Houée-Levin, C. (2001) *FEBS Lett. 497*, 171−173.
19. Abreu, I. A., Saraiva, L. M., Soares, C. M., Teixeira, M., and Cabelli, D. E. (2001) *J. Biol. Chem. 276*, 38995−39001.
20. Emerson, J. P., Coulter, E. D., Cabelli, D. E., Phillips, R. S., and Kurtz, D. M., Jr (2002) *Biochemistry 41*, 4348−4357.
21. Mathé, C., Mattioli, T. A., Horner, O., Lombard, M., Latour, J. M., Fontecave, M., and Nivière, V. (2002) *J. Am. Chem. Soc. 124*, 4966−4967.
22. Horner, O. et al. (2003) manuscript submitted.
23. Silaghi-Dumitrescu, R., Silaghi-Dumitrescu, I., Coulter, E. D., and Kurtz, D. M., Jr. (2003) *Inorg. Chem. 42*, 446−456.
24. Berthomieu, C., Dupeyrat, F., Fontecave, M., Verméglio, A., and Nivière, V. (2002) *Biochemistry 41*, 10360−10368.
25. Pianzzola, M. J., Soubes, M., and Touati, D. (1996) *J. Bacteriol. 178*, 6736−6742.
26. Jouanneau, Y., Meyer, C., Asso, M., Guigliarelli, B., and Willison, J. C. (2000) *Eur. J. Biochem. 267*, 780−787.
27. Favaudon, V., Tourbez, H., Houée-Levin, C., and Lhoste, J. M. (1990) *Biochemistry 29*, 10978−10989.
28. Schuler, R. H., Patterson, L. K., and Janata, E. (1980) *J. Phys. Chem. 84*, 2088−2089.
29. Von Sonntag, C. (1987) *The Classical Basis of Radiation Biology*, Taylor and Francis, London.
30. Bielski, B. H. L., Cabelli, D. E., Arudi, R. L., and Ross, A. B. (1985) *J. Phys. Chem. Ref. Data 14*, 1041−1097.
31. Clay, M. D., Jenney, F. E., Jr., Noh, H. J., Hagedoorn, P. L., Adams, M. W. W., and Johnson, M. K. (2002) *Biochemistry 41*, 9833−9841.

BI035698I